**Climate
of the Past
Discussions**

Impact of postglacial warming on borehole reconstructions of last millennium temperatures

V. Rath[1], J. F. González Rouco[1], and H. Goosse[2]

[1]Universidad Computense de Madrid, Facultad CC. Físicas, Departamento de Astrofísica y CC de la Atmosfera, Ciudad Universitaria, 28040 Madrid, Spain
[2]Centre de recherches sur la terre et le climat Georges Lemaître, Earth and Life Institute, Université Catholique de Louvain, 2 chemin du Cyclotron, 1348 Louvain-la-Neuve, Belgium

Correspondence to: V. Rath (vrath@fis.ucm.es)

CPD

7, 3325–3347, 2011

Subsurface impact of postglacial warming

V. Rath et al.

Subsurface impact of postglacial warming

V. Rath et al.

Abstract

The investigation of observed borehole temperatures has proved to be a valuable tool for the reconstruction of ground surface temperature histories. However, there are still many open questions concerning the significance and accuracy of the reconstructions from these data. In particular, the temperature signal of the warming after the Last Glacial Maximum is still present in borehole temperature profiles. It is shown here that this signal also influences the relatively shallow boreholes used in current paleoclimate inversions to estimate temperature changes in the last centuries by producing errors in the determination of the steady state geothermal gradient. However, the impact on estimates of past temperature changes is weaker. For deeper boreholes, the curvature of the long-term signal is significant. A correction based on simple assumptions about glacial-interglacial temperature changes shows promising results, improving the extraction of millennial scale signals. The same procedure may help when comparing observed borehole temperature profiles with the results from numerical climate models.

1 Introduction

In steady-state thermal conditions at the surface, the subsurface geothermal gradient, neglecting heat production, can be approximated by a linear profile (e.g. Pollack and Huang, 2000). If perturbations in surface temperatures occur, they propagate to the subsurface and deform the geothermal gradient. Such deviations are registered by borehole temperature profiles (BTPs) and have been successfully used to reconstruct ground surface temperature histories (GSTHs), providing estimates of preindustrial-to-present temperature change that complement those of other proxy reconstructions (e.g. Jansen et al., 2007). Nevertheless, there is still a number of open questions concerning possible biases in borehole based reconstructions (e.g. Smerdon et al., 2006; Wilhelm et al., 2005; Verdoya et al., 2007; Mottaghy and Rath, 2006), making

the choice of boreholes, the careful evaluation of their setup, and a valid treatment of the data a considerable task for the interpreter.

One of such uncertainty sources concerns the potential effect of long term surface perturbations like the warming from the Last Glacial Maximum (LGM) to the Holocene. Though reliable conclusions about the last 25 000 years can only be drawn using sub-surface temperatures from the rare deep boreholes with depths of 2000 m and more (e.g. Chouinard and Mareschal, 2009), at shallower depths of less than 1000 m, the post-LGM warming may also leave an imprint through smooth changes of the temper-ature gradient. Within this depth domain, there is an abundance of BTPs which could be a valuable source of information on the last millennium and late Holocene. The extent to which such perturbations can affect the interpretation of past temperature inversion from BTPs within this range of depths is unclear.

Since the times of Birch (1948), corrections for paleoclimate effects have been pro-posed and applied when estimating heat flow densities (e.g. Vasseur and Lucazeau, 1983; Majorowicz and Wybraniec, 2010), though this is not yet the standard proce-dure (Davies and Davies, 2010). Surprisingly, the role of postglacial warming in the reconstruction of past climates has not yet been studied systematically, though its effect was identified as a source of error when inverting very shallow borehole tem-perature profiles many times (amongst others Majorowicz, 2004; Hartmann and Rath, 2005; Beltrami et al., 2011). In this paper we show that the analysis of its impact is even more important when interpreting deeper boreholes. Important implications may be expected not only for derived temperatures, stored heat, and heat flow estimations, but also when comparing observed BTPs and model simulations (see González-Rouco et al., 2009, and references therein). Therefore, it would be highly desirable to estimate the influence of postglacial warming on BTPs of variable depths within the first km of the subsurface and, if possible, formulate approaches for dealing with this situation.

This work analyzes these issues by performing Monte-Carlo simulations with a one-dimensional forward modeling code under plausible glacial-interglacial surface temper-ature forcing conditions described in Sect. 2. This allows to illustrate the effects of

postglacial warming on shallow BTPs and to develop simple corrections that mitigate their induced errors in Sect. 3. In Apendices A to C we give further information on the numerical procedure which we used to produce the Monte Carlo (MC) results, the inverse procedure employed, and some additional figures.

2 Monte-Carlo simulations

In order to give a quantitative estimate of the effect of the postglacial temperature rise, Monte-Carlo (MC) simulations were performed. For these we employed a simple numerical one-dimensional forward modeling code (Mottaghy and Rath, 2006; Rath and Mottaghy, 2007), which is described in more detail in Appendix A. To represent the past temperature variations, a simplified upper temperature boundary was used. It is based on a sequence of step functions as shown in Fig. 1. The parameters sampled in the MC calculations are the times of temperature changes t_1 and t_2, and the corresponding temperature deviations ΔT_1 and ΔT_2, respectively. ΔT_1 may be described as the temperature rise between glacial and Holocene conditions, while ΔT_2 represents the difference between Holocene and the long-term Quaternary mean. We assumed parameter distributions for location and amplitude of both step functions, as well as for the petrophysical properties,the thermal conductivity and the volumetric heat capacity, λ_m and $(\rho c)_m$ of the rock, respectively. The general shape of the step functions shown in Fig. 1 was qualitatively motivated by estimations like those of GRIP, EPICA and Vostok (e.g. NGRIP Working Group, 2004; Jouzel et al., 2007). The values are within the uncertainties of present knowledge concerning glacial to interglacial land temperature change, and embrace scenarios of less cooling like those plausibly suffered at lower latitudes as well as larger temperature changes registered in proxy data and simulated by models for northern latitudes (Jansen et al., 2007; Otto-Bliesner et al., 2009, and references therein). Some large temperature changes over land (e.g. Jost et al., 2005) were assigned low probabilities. The choice of GSTH also would not include sites from the very high latitudes, where the conditions at the base of the ice sheets may cause LGM ground surface temperatures significantly higher than during the Holocene.

Title Page

Abstract | Introduction

Conclusions | References

Tables | Figures

◄ | ►

◄ | ►

Back | Close

Full Screen / Esc

Printer-friendly Version

Interactive Discussion

The boundary conditions of Fig. 1 do not intend to be exhaustive in including all potential past climate trajectories, but to provide a plausible framework of temperature change over typical borehole locations that can be used to demonstrate their effect on BTPs. Obviously, if better information is available on the regional climate conditions during the last glacial cycle, the probable signature of GST changes can be constrained accordingly.

The resulting six parameters were assumed to be independently distributed following a Normal distribution $\mathcal{N}(\hat{\mu}, \hat{\sigma})$. The values assumed for the means $\hat{\mu}$ and standard deviations $\hat{\sigma}$ are given in Appendix A. This set of parameters was randomly sampled, producing an ensemble of 10 000 runs of the forward modeling code.

Figure 2 shows the difference of the resulting BTPs with respect to the reference, i.e. a constant GSTH of $T_s = 6\,^\circ$C implying steady-state conditions. The results indicate that the temperature profiles differ considerably from the reference by the influence of the earlier temperature changes. The largest deviations in temperature occur at depths between 1000 m and 1500 m. Clearly, the true steady state condition can not easily be estimated from the temperature and thermal properties alone for a given shallow (say, <500 m) borehole, as it is often done in practice by assuming that the quasi-linear bottom part of the profile represents the geothermal gradient. This may be concluded from the observation that the vertical temperature gradient approaches its true value only at depths near 2000 m. It follows, that under most probable conditions, results of GSTH inversions could be influenced by this transient effect mistaken for a steady-state component. Additionally, this implies that differences in log depth may falsely translate into different geothermal gradients, and in consequence, GST histories.

3 A simple correction approach

Boreholes of less than 1000 m depth allow targeting changes of the last several 1000 yrs. It is highly desirable, however, to make better use of the information content of these shallow BTPs, as they are abundant in many areas, while deep boreholes are

very rare. Therefore a simple procedure is proposed, by which shorter BTPs may be corrected for the influence of the glacial-interglacial transition with just an approximate knowledge of the regional long-term paleo-temperatures.

A GSTH based on the major features of the Holocene warming scenario with addi-
5 tional temperature variations during the last 500 yrs (grey line in Fig. 3) was used to generate synthetic BTPs of different depth between 250 m and 1250 m. This scenario includes a Little Ice Age (LIA) like minimum around ca. 1700 and a warming of about half a degree in the last century. After being artificially perturbed with noise, these synthetic observations were interpreted using a regularized linear inversion scheme (see
10 Beltrami and Mareschal, 1991; Mareschal and Beltrami, 1992, SM). Results show a large variability among the inverted BTPs (Fig. 3), particularly before the LIA minimum where deviations to the reference GSTH can reach about half a degree at the beginning of the millennium. This discrepancy mainly arises because of the post-glacial warming that fakes true temperature changes in the last millennium. This can then be corrected
15 by subtracting the response corresponding to the long term component of the GSTH, which is the original GSTH with a constant temperature assumed from 12 000 years BP onward (see Fig. 1, red line). This leads to much more consistent results for all inverted profiles for all of the millennium (Fig. 3).

Concerning the use of shallow (say, <500 m) boreholes, it has to be noted, that sin-
20 gle shallow boreholes usually still lead to significant short term reconstructions that reproduce the changes in the last centuries, because the disturbing temperature signal is nearly linear, and can thus easily be represented by an erroneous steady state component (i.e. the geothermal gradient) of the model. This can easily be seen in Fig. 4, where estimated background heat flow estimated from BTPs of increasing depths is
25 shown for a realistic profile including the post LGM warming (red), and its corrected version (green) as well as for a case including only changes in the last millennium (green; excluding post LGM warming), and for the steady state (gray). The background geothermal gradients derived from the raw profile (i.e. including LGM effects) at shallow depths are systematically too low, while the ones derived from the corrected values are

very similar to the true ones. They also agree with the results for synthetic BTPs estimated from a reference GSTH, which is constant in time with exception of the millennial period.

For this reasons, increasing the depth into the domain of changing vertical gradi-
⁵ ent will not generally improve results. In this case, the effect of the Holocene warming may not be treated as a simple offset in basal heat flow density, but will produce an erroneous signal in the whole profile, and therefore in the reconstructed surface temperatures. If BTPs of different depths are compared, or even interpreted jointly, inconsistencies and corresponding errors in the results will arise.

¹⁰ Clearly, the method as applied here makes use of our prior knowledge of long term GSTH, and to less extent on rock properties and basal heat flow as far as nonlinearity has to be considered. However, it turns out that the results can also be improved by using approximate information. Sensitivity tests (some given in Appendix C) indicate that even inaccurate long-term models improve inversion results considerably.

¹⁵ Note that for this case involving an abrupt change in temperature, all inverted GSTHs, whether corrected or not, underestimate the temperature change in the last 1000 yrs. This is due to the existence of many GSTH leading to a similar fit of the observations. The inverse problem is ill-posed (Hansen, 1998, 2010), and can only be solved by regularization. The particular method used here, is based on a damped
²⁰ singular value decomposition. As many other commonly employed methods, it will lead to smooth solutions which will not reproduce abrupt changes like the one we have chosen for the numerical experiment. If the corresponding regularization parameter is chosen properly (see Appendix B), the effect of postglacial warming would not lead to a general overestimation of variation. Such overestimation would have explained the
²⁵ comparatively cold temperatures of the borehole reconstruction results presented by Jansen et al. (2007); the present numerical experiments, however, indicate that this hypothesis is not valid.

Additionally, it should be noted that this simple reduction approach is not the only possible one when reconstrucing past surface temperature changes. In the case of Bayesian-type reconstruction algorithms (see, e.g. Tarantola, 2005), the earlier surface temperature changes could be introduced as a prior model in the case of a gaussian maximum aposteriori estimate, or included into the prior probabilty distribution in the more general case.

4 Impact for model-observation comparison

A similar problem may result when comparing the output of AOGCM simulations with field data (Stevens et al., 2008). AOGCM simulations on millennial scale usually start with initial conditions assuming steady state conditions in the subsurface. Due to the long temperature memory of the subsurface, this is not the case.

When comparing AOGCM outputs with borehole data, the standard procedure with BTPs is estimating perturbations from a reference geothermal gradient, and assuming equilibrium heat flow in the deeper part of the observed BTP. These perturbation profiles (often called reduced temperatures) are then compared with the results of using modeled surface air temperature (SAT) as top boundary condition for the thermal subsurface model.

Here, the same situation applies as with inversion. In the case of shallow boreholes, a reasonable background heat flow (including the steady-state and long period component) may be estimated by an appropriate procedure, e.g. the inverse approach used above above, depending on prior site knowledge. For deeper boreholes, the curvature of LGM-influenced BTPs is significant. Therefore the correction approach explained in Sect. 3 should improve results considerably. It must be re-iterated, that this approach depends on assumed prior knowledge on long-term climate, implying that care has to be taken when choosing this GSTH. This is particularly important when comparing BTPs to simulation outputs implies moving from global scale to regional studies.

5   Conclusions

From the simple modeling studies presented above a few conclusions may be drawn. First of all, the signature of the LGM and Holocene warming can not be neglected even in shallow boreholes. In this case, however, the nearly linear behavior of the LGM-derived signal component can be emulated by an erroneous background equilibrium heat flow. In the case of deeper BTPs, carrying informations from times before the LIA, the curvature of the perturbing signal becomes important, and differences in depth translate to variations in inferred paleo-temperatures. In the same way, reduced temperatures calculated for comparison with GCM output may be biased. A first order correction, however, seems possible by means of approximate knowledge on prior development of surface temperatures. The power of this approach has of course to be investigated in the field, which remains a task for the future.

Appendix A

Supplementary information on the MC simulation

The one-dimensional, purely conductive heat equation in a porous medium can be written as:

$$\frac{\partial}{\partial z}\left(\lambda_e \frac{\partial T}{\partial z}\right) + h = (\rho c)_e \frac{\partial T}{\partial t}, \tag{A1}$$

where λ is thermal conductivity ($\mathrm{Wm^{-1}K^{-1}}$), (ρc) is the volumetric heat capacity ($\mathrm{JK^{-1}m^{-3}}$), and h is volumetric heat production ($\mathrm{Wm^{-3}}$). The subscript e marks effective parameters of the porous medium, and can be interpreted as properties of a two-phase mixture between solid rock and fluid-filled pore space. For the paleoclimate application we have in mind, Eq. (A1) usually is solved with appropriate boundary

conditions, namely fixed but time-dependent temperature $T = T(t)$ at the top, $z = z_0$, and fixed heat flow density q_b at the base at $z = z_b$.

Equation (A1) is understood to allow all coefficients, boundaries, and sources, to be nonlinearly dependent on temperature. As we are aiming at deep boreholes recording the history of ground surface temperature for some 10 000 years, we have to extend the numerical model to depths of several 1000 m for numerical reasons and temperatures of up to 200 °C accordingly. This requires taking the temperature dependencies of the thermophysical properties into account, possibly including phase change by freezing and thawing of pore water. Details of theory, implementation, and the validation of the approach can be found in Mottaghy and Rath (2006) and Rath and Mottaghy (2007). In contrast, if aiming at millennial scale events as the little ice age in Europe, analytical models (e.g. Beltrami and Mareschal, 1991; Mareschal and Beltrami, 1992, used in the inverse experiments described below) assuming constant properties are often sufficient for the interpretation of BTPs, implying additivity of solutions.

The parameter choices for the MC simulations are given in Table 1. While the rock parameters λ_m and $(\rho c)_m$ are plausible for the most common crustal rocks. To complete the model set up, we have assumed a moderate porosity of $\phi = 0.1$, a recent surface temperature of $T_s = 6$ °C, and a heat flow density of 50 mW m^{-2}.

The software to produce the results presented in the main article may be downloaded from the first author's web page (http://palma.fis.ucm.es/~volker/MC_web.tar.gz).

Appendix B

Additional information on the inverse numerical experiments

For the numerical experiments on GSTH inversion, we used a commonly employed procedure (Beltrami and Mareschal, 1991; Mareschal and Beltrami, 1992; Beltrami et al., 1995; Clauser and Mareschal, 1995), where a simple analytical forward solution is

used, and the subsurface is assumed to be homogeneous:

$$T(z,t) = T_0 + \frac{q_0 z}{\lambda} - \frac{A z^2}{2\lambda} + T_t(z,t) \tag{B1}$$

The first three terms represent the steady-state component, defined by the heat flow density at the surface q_0, the equilibrium ground surface temperature T_0, the constant
5 thermal conductivity λ, and heat production rate A of the subsurface, which in most cases can safely be neglected. If the GST history is parameterized by a series of temperature steps T_j^G at times t_j before present ($t = 0$), the remaining transient temperature term $T_t(z,t)$ at time t and depth z is given by (Carslaw and Jaeger, 1959):

$$T_t(z) = \sum_{j=1}^{N} T_j^G \left(\operatorname{erfc}\left(\frac{z}{2\sqrt{\kappa t_j}} \right) - \operatorname{erfc}\left(\frac{z}{2\sqrt{\kappa t_{j-1}}} \right) \right) \tag{B2}$$

10 If $T_t(z) = T_t(z_i)$ is given at discrete depths i, a corresponding linear inverse problem for the T_j^G, T_0, and q_0 can be formulated. In the cases shown, 20 temperature steps logarithmically equispaced between 10 yrs b.p. and 1000 yrs b.p. were used. To deal with the inherent ill-posedness of this problem (Hansen, 2010), it is solved using a truncated singular value decomposition approach as described by Mareschal and Beltrami
15 (1992). In order to keep the numerical experiment free of the ambiguities when choosing the necessary regularization parameter, a constant ϵ was determined beforehand by the L-curve method (Hansen, 1998, 2010). For all depths considered here, a value of $\epsilon = 0.3$ seemed appropriate. Individual determination of the regularization parameter for each temperature profile does not produce fundamentaly different results.
20 To eludicate the generally smoothing behavior of this algorithm, a simple numerical experiment assuming a GSTH of constant value before the LIA is presented here. For the numerical experiments we used the GSTHs shown in Fig. 5, random perturbation were added to the original simulated data, assuming a normal distribution $\mathcal{N}(\hat{\mu}, \hat{\sigma})$

with $\hat{\mu} = 0$ and standard deviations $\hat{\sigma} = 0.1$ K. Noise correlation was produced using a rectangular linear filter of length 5.

The results for different choices of the regularization parameter ϵ are given in Fig. 6a. The overall smoothing behavior of this regularized inversion is evident. Additionally, the L-curve for this experiment is shown in Fig. 6b. While at small regularization parameters (e.g. $\epsilon = 0.03$, blue), the inverted GST shows overshoots, and a behavior strongly dependent on noise in the observations, higher values (e.g. $\epsilon = 0.3$) will lead to stable, but oversmoothing behavior. This is well reflected in the L-curve (Hansen, 2010) on the right, which has its corner somewhere between $\epsilon = 0.4$ and $\epsilon = 0.1$. As common in ill-posed inverse problems, a trade-off between data fit and stability of results can be obtained near the corner of the L-curve.

The MATLAB™ scripts used for the inverse experiments presented in the main article and here may be downloaded from the first author's web page (http://palma.fis.ucm.es/~volker/GSTHinvA_web.tar.gz).

Appendix C

Senstivity studies for the correction approach

To give examples, Fig. 7 shows results obtained by varying the prior GSTH calculating the correction applied to the raw data. In the first case a ±2.5 K deviation of the minimal temperatures at the LGM were used, assumed to be lower than the recent GST by a ΔT of -5 K. In the second, the time of postglacial warming (12 Kyrs b.p.) is modified by ±2 kyrs. The differences between the inferred GST histories are much smaller than in the case of uncorrected observations. Similar results are obtained for the other parameters. These result indicate that even incomplete prior knowledge on paleo-temperatures may improve consistency and realism of the inversion results.

References

Beltrami, H. and Mareschal, J.-C.: Recent warming in eastern Canada inferred from Geothermal Measurements, Geophys. Res. Lett., 18, 605–608, 1991. 3330, 3334

Beltrami, H., Chapman, D. S., Archambault, S., and Bergeron, Y.: Reconstruction of high resolution ground temperature histories combining dendrochronological and geothermal data, Earth Planet. Sci. Lett., 136, 437–445, 1995. 3334

Beltrami, H., Smerdon, J. E., Matharoo, G. S., and Nickerson, N.: Impact of maximum borehole depths on inverted temperature histories in borehole paleoclimatology, Clim. Past, 7, 745–756, doi:10.5194/cp-7-745-2011, 2011. 3327

Birch, F.: The Effects of Pleistocene Climatic Variations upon Geothermal Gradients, American Journal of Science, 246, 729–760, 1948. 3327

Carslaw, H. S. and Jaeger, J. C.: Conduction of heat in solids, Oxford Univ. Press. 2nd ed., New York, 3rd. edn., 1959. 3335

Chouinard, C. and Mareschal, J.-C.: Ground surface temperature history in southern Canada: Temperatures at the base of the Laurentide ice sheet and during the Holocene, Earth Planet. Sc. Lett., 277, 280–289, 2009. 3327

Clauser, C. and Mareschal, J.-C.: Ground temperature history in central Europe from borehole temperature data, Geophys. J. Int., 121, 805–817, 1995. 3334

Davies, J. H. and Davies, D. R.: Earth's surface heat flux, Solid Earth, 1, 5–24, doi:10.5194/se-1-5-2010, 2010. 3327

González-Rouco, J. F., Beltrami, H., Zorita, E., and Stevens, M. B.: Borehole climatology: a discussion based on contributions from climate modeling, Clim. Past, 5, 97–127, doi:10.5194/cp-5-97-2009, 2009. 3327

Hansen, P. C.: Rank Deficient and Discrete Ill-Posed Problems, SIAM, Philadelphia, 1998. 3331, 3335

Hansen, P. C.: Discrete Inverse Problems. Insight and Algorithms, SIAM, Philadelphia PA, 2010. 3331, 3335, 3336, 3346

Hartmann, A. and Rath, V.: Uncertainties and shortcomings of ground surface temperature histories derived from inversion of temperature logs, Journal of Geophysics and Engineering, 2, 299–311, doi:10.1088/1742-2132/2/4/S02, 2005. 3327

Jansen, E., Overpeck, J., Briffa, R., Duplessy, J.-C., Joos, F., Masson-Delmotte, V., Olago, D., Otto-Bliesner, B., Peltier, W., Rahmstorf, S., Ramesh, R., Raynaud, D., Rind, D., Solomina,

Title Page

Abstract | Introduction

Conclusions | References

Tables | Figures

◄ | ►

◄ | ►

Back | Close

Full Screen / Esc

Printer-friendly Version

Interactive Discussion

O., Villalba, R., and Zhang, D.: Palaeoclimate, in: Climate Change 2007: The Physical Science Basis, edited by: Solomon, S., Qin, D., Manning, M., Chen, Z., Marquis, M., Averyt, K., Tignor, M., and Miller, H., Cambridge University Press, Cambridge, UK and New York, NY, USA, 2007. 3326, 3328, 3331

5 Jost, A., Lunt, D., Kageyama, M., Abe-Ouchi, A., Peyron, O., and G. Ramstein: High-resolution simulations of the last glacial maximum climate over Europe: a solution to discrepancies with continental palaeoclimatic reconstructions, Clim. Dynam., 24, 577–590, doi:10.1007/s00382-005-0009-4, 2005. 3328

Jouzel, J., Masson-Delmotte, V., Cattani, O., Dreyfus, G., Falourd, S., Hoffmann, G., Minster,
10 B., Nouet, J., Barnola, J., Chappellaz, J., Fischer, H., Gallet, J., Johnsen, S., Leuenberger, M., Loulergue, L., Luethi, D., Oerter, H., Parrenin, F., Raisbeck, G., Raynaud, D., Schilt, A., Schwander, J., Selmo, E., Souchez, R., Spahni, R., Stauffer, B., Steffensen, J., Stenni, B., Stocker, T., Tison, J., Werner, M., and Wolff, E.: Orbital and Millennial Antarctic Climate Variability over the Past 800,000 Years, Science, 317, 793–797, 2007. 3328, 3341

15 Majorowicz, J. A.: Thermal lithosphere across the Trans-European Suture Zone in Poland, Geological Quarterly, 49, 1–14, 2004. 3327

Majorowicz, J. and Wybraniec, S.: New terrestrial heat flow map of Europe after regional paleoclimatic correction application, International Journal of Earth Sciences, published online, doi:10.1007/s00531-010-0526-1, 2010. 3327

20 Mareschal, J.-C. and Beltrami, H.: Evidence for recent warming from perturbed thermal gradients: examples from eastern Canada, Clim. Dynam., 6, 135–143, 1992. 3330, 3334, 3335

Mottaghy, D. and Rath, V.: Latent heat effects in subsurface heat transport modeling and their impact on paleotemperature reconstructions, Geophys. J. Int., 164, 236–245, doi:10.1111/j.1365-246X.2005.02843.x, 2006. 3326, 3328, 3334

25 NGRIP Working Group: High-resolution record of Northern Hemisphere climate extending into the last interglacial period, Nature, 431, 147–151, 2004. 3328

Otto-Bliesner, B., Schneider, R., Brady, E. C., Kucera, M., Abe-Ouchi, A., Bard, E., Braconnot, P., Crucifix, M., Hewitt, C. D., Kageyama, M., Marti, O., Paul, A., Rosell-Melé, A., Waelbroeck, C., Weber, S. L., Weinelt, M., and Yu, Y.: A comparison of PMIP2 model simulations and the
30 MARGO proxy reconstruction for tropical sea surface temperatures at last glacial maximum, Clim. Dynam., 32, 799–815, 2009. 3328

Pollack, H. N. and Huang, S.: Climate reconstruction from subsurface temperatures, Annu. Rev. Earth. Planet. Sci., 28, 339–365, 2000. 3326

Rath, V. and Mottaghy, D.: Smooth inversion for ground surface temperature histories: estimating the optimum regularization parameter by generalized cross-validation, Geophys. J. Int., 171, 1440, doi:10.1111/j.1365-246X.2007.03587.x, 2007. 3328, 3334

Smerdon, J. E., Pollack, H. N., Cermak, V., Enz, J. W., Kresl, M., Šafanda, J., and Wehmiller, J. F.: Daily, seasonal and annual relationships between air and subsurface temperatures, J. Geophys. Res., 111, D07101, doi:10.1029/2004JD005578, 2006. 3326

Stevens, M. B., González-Rouco, J. F., and Beltrami, H.: North American climate of the last millennium: Underground temperatures and model comparison, J. Geophys. Res., 113, F01008, doi:10.1029/2006JF000705, 2008. 3332

Tarantola, A.: Inverse problem theory. Methods for model parameter estimation, SIAM, Philadelpha, http://www.ipgp.jussieu.fr/~tarantola/Files/Professional/Books/index.html, 2005. 3332

Vasseur, G. and Lucazeau, F.: Bounds on paleotemperatures and paleoclimatic corrections, Zentralbl. Geol. Paleontol., 1, 17–24, 1983. 3327

Verdoya, M., Chiozzi, P., and Pasquale, V.: Thermal log analysis for recognition of ground surface temperature change and water movements, Clim. Past, 3, 315–324, doi:10.5194/cp-3-315-2007, 2007. 3326

Wilhelm, H., Popov, Y., Burkhardt, H., Šafanda, J., Čermák, V., Heidinger, P., Korobkov, D., Romushkevich, R., and Mayr, S.: Heterogeneity effects in thermal borehole measurements in the Chicxulub impact crater, Journal of Geophysics and Engineering, 2, 357–363, doi:10.1088/1742-2132/2/4/S09, 2005. 3326

Table 1. Parameters used for the Monte-Carlo simulations in this study. They were assumed to be independently and normally distributed. λ_m and $(\rho c)_m$ are the rock matrix properties.

	λ_m ($\frac{W}{mK}$)	$(\rho c)_m$ ($\frac{MJ}{kgK}$)	ΔT_1 (K)	Δt_1 (kyr)	ΔT_2 (K)	Δt_2 (kyr)
$\hat{\mu}$	2.5	2.0	5.5	14	4	80
$\hat{\sigma}$	0.5	0.5	2	2	2	10
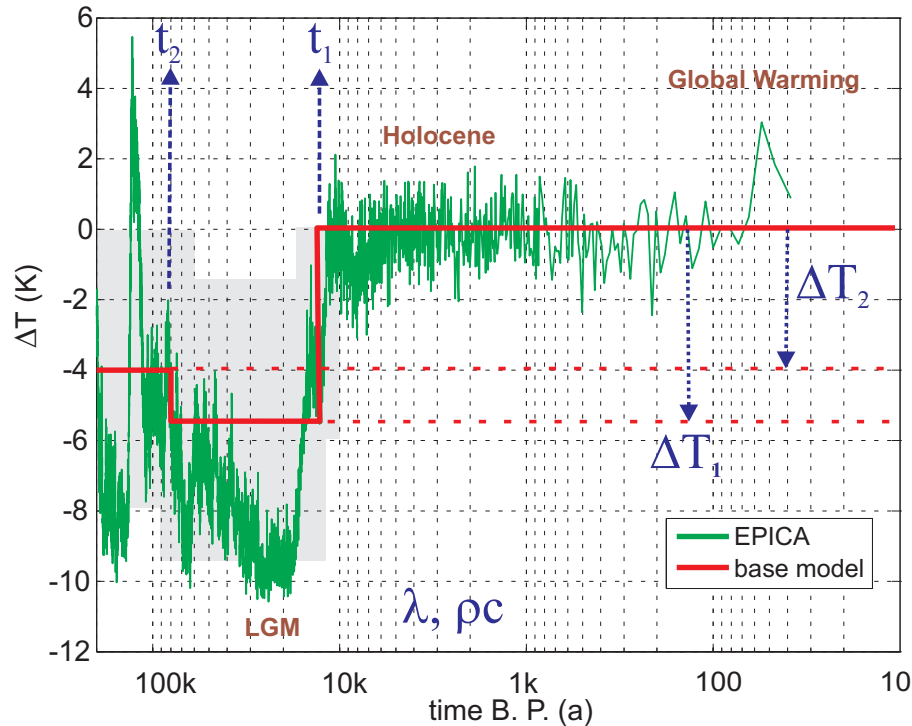
Fig. 1. GSTH forcing used for the calculations presented in this study. Also shown are the parameters and their variations used for the Monte Carlo investigations. $2\hat{\sigma}$ boundaries are marked by grey shades. The general shape of the GSTH for this numerical experiment is motivated by the EPICA ice core reconstructions (Jouzel et al., 2007). Note that the base model is constant since the postglacial temperature rise.
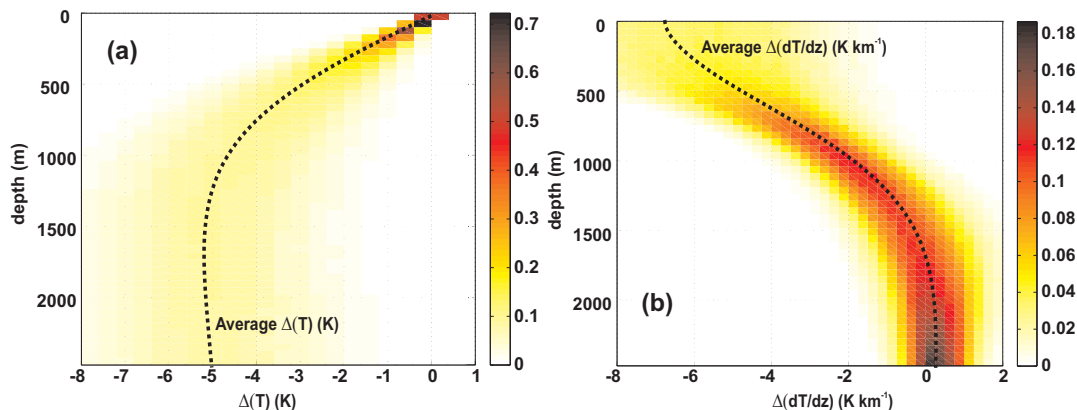
Fig. 2. Results of the Monte Carlo study. Normalized histogram densities of the temperature deviation calculated for the long-term models with reprect to steady-state conditions **(a)**, and their vertical derivative **(b)** as functions of depth. The integral along the x axis is equal to 1 for all depth, as the densities are normalized by the number of runs (10 000).
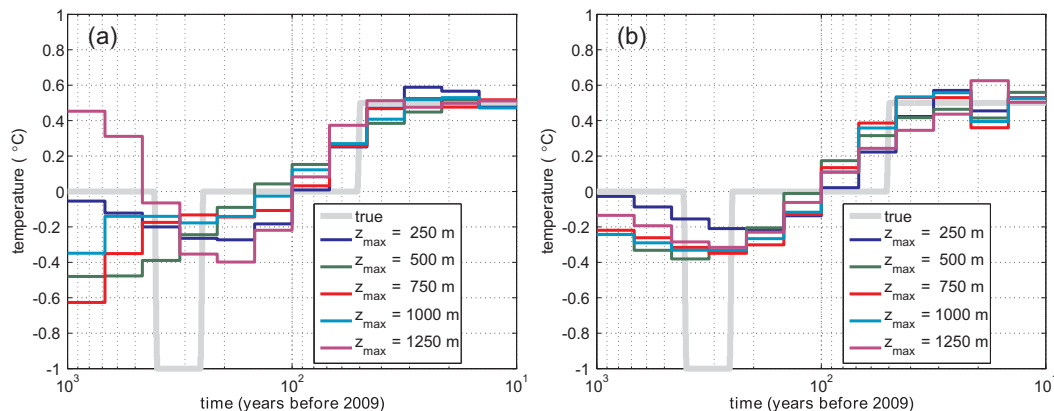
Fig. 3. Using prior knowledge for correction of shallow borehole temperature profiles. **(a)** Inversion of BTP of different lengths derived from a synthetic GSTH (shown in grey), which shows constant temperatures since the postglacial temperature rise. **(b)** Boreholes were corrected by subtracting the response to this prior GSTH. The shallowest BTP (250 m, dark blue) is too short to resolve the LIA-like structure, and thus the results show only very weak effects, independent of whether input data are raw or corrected.

Title Page

Abstract | Introduction

Conclusions | References

Tables | Figures

|◄ | ►|

◄ | ►

Back | Close

Full Screen / Esc

Printer-friendly Version

Interactive Discussion
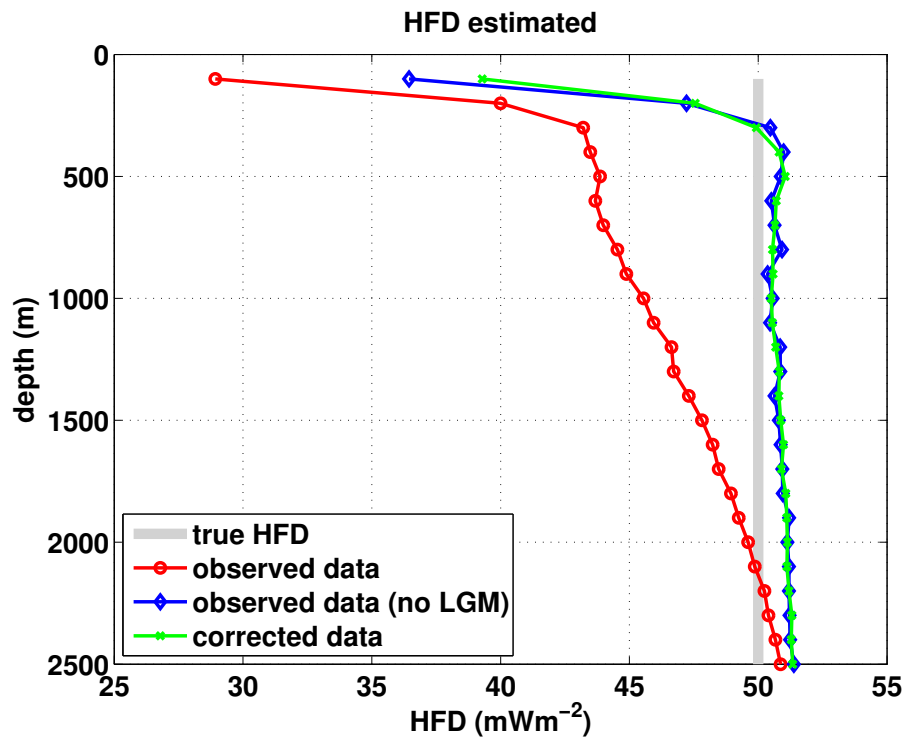
Fig. 4. Background heat flow density values obtained as a result from inverting original synthetic (red), synthetic data without LGM (blue), and corrected data (green). Obviously, in the first case the estimated heat flow density is the superposition of the nearly linear equilibrium component, and the effect of post-glacial warming. Shown in grey is the true constant value. The remaining deviation from the true one is present in the blue and green curve. It depends on the observations, their errors, and the choice of the regularization parameter.
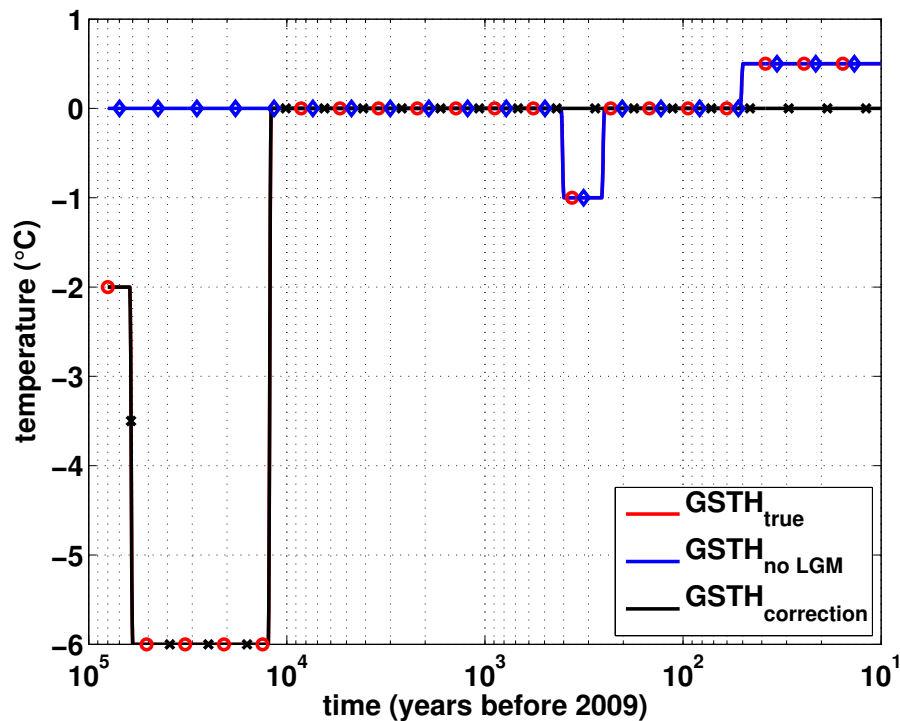
Fig. 5. GSTH used in the synthetic inversion experiments. BTPs derived from the true model (red) are named observed data, while the temperatures used for correction are derived from the black GSTH. for comparison, also synthetic observations assuming a constant behavior before the LIA.
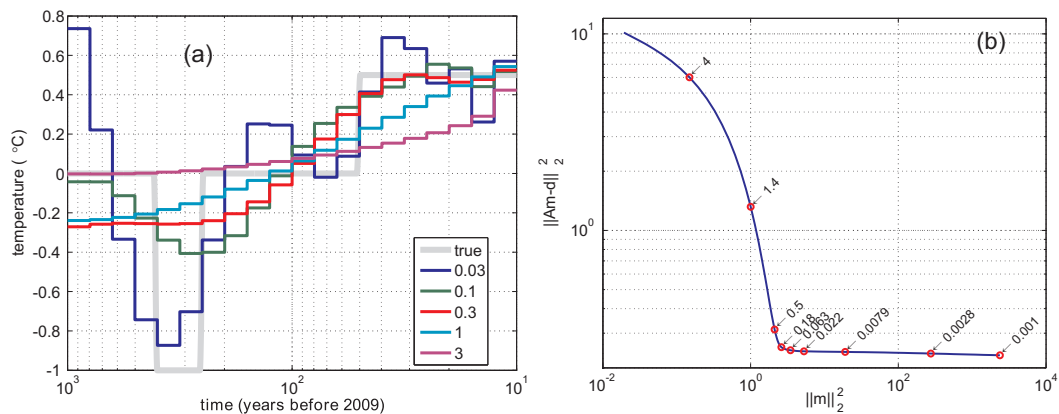
Fig. 6. Inversions of borehole temperature profiles for a fixed depth (500 m), where a GSTH of constant value before the LIA is assumed. Results for different values of the regularization paramter are shown in **(a)**. The corresponding L-curve (Hansen, 2010) is shown in panel **(b)**.
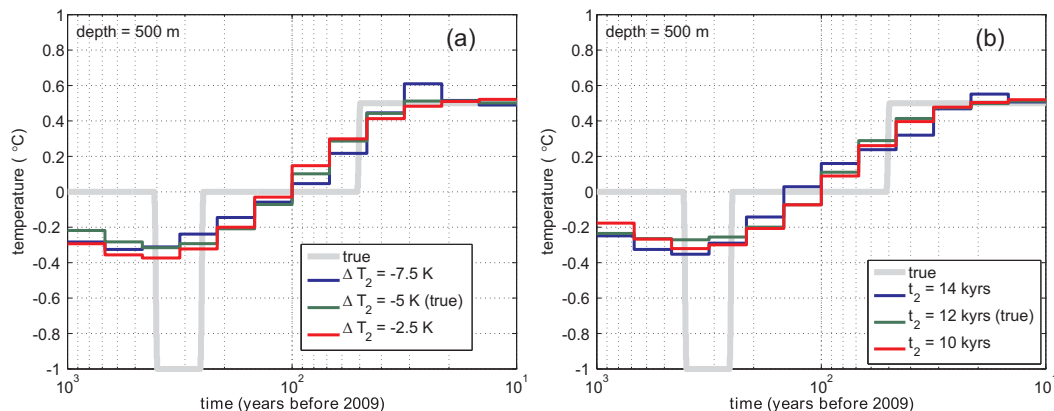
Fig. 7. Sensitivities of corrections with respect to assumed amplitude of LGM temperatures. Inverted BHT from a BTP with a length of 500 m. Data were corrected with different paleo-temperature scenarios, with maximal temperature steps of $\Delta T_1 5 \pm 2.5$ K **(a)**, and the corresponding step times $t_1 12 \pm 2$ kyrs (right).